Role of oxygen nonstoichiometry and the reduction process on the local structure of $Nd_{2-x}Ce_xCuO_{4\pm\delta}$

P. Richard,* G. Riou, I. Hetel, S. Jandl, M. Poirier, and P. Fournier
Regroupement Québécois sur les Matériaux de Pointe, Département de Physique, Université de Sherbrooke, Sherbrooke, Canada J1K 2R1

(Received 9 March 2004; revised manuscript received 10 June 2004; published 25 August 2004)

We report Raman and crystal-field infrared transmission studies of $Nd_{2-x}Ce_xCuO_4$ single crystals. Nd^{3+} crystal-field excitations from the ground state to excited multiplets are detected. While the Nd^{3+} regular site is almost not perturbed by Ce-doping and oxygen nonstoichiometry, oxygen vacancies in O(1) and O(2) sites, as well as apical oxygen, are detected. The type of oxygen vacancies created is found to be Ce-doping dependent, with the reduction of the optimally doped samples involving only CuO_2 plane O(1) oxygen vacancies. In contrast to the widespread belief, the apical oxygen is not removed by the reduction of as-grown samples.

DOI: 10.1103/PhysRevB.70.064513 PACS number(s): 74.72.Jt, 71.70.Ch

I. INTRODUCTION

Since their discovery, the 2-1-4 electron-doped superconductors $RE_{2-x}Ce_xCuO_4$, RE=Pr,Nd,Sm (Ref. 1) occupy a particular status among all cuprates. Contrary to the other cuprates, the substitution of RE^{3+} by Ce^{4+} in these materials is known to inject electrons instead of holes into the CuO_2 planes. Moreover, as-grown Ce-doped samples become superconductors only after reduction. The belief that the removal of a small amount of extraneous oxygen above copper [apical oxygen O(3)], explaining the appearance of superconductivity in reduced samples, is widely spread. The oxygen content influences many important parameters such as T_c, the concentration of free carriers, their mobility and their scattering rate.[2] As suggested by theoretical considerations[3] and Hall coefficient measurements,[4–8] it also affects the charge character of the carriers. A positive contribution to the Hall coefficient, increased by doping, is observed in reduced optimally doped and overdoped samples.[8] Consequently, the role and the mechanism of the reduction process which triggers the superconductivity seems more complex than expected. The understanding of the local crystallographic structure and charge distribution modified by the oxygen nonstoichiometry is crucial to the comprehension of the so-called electron-doped compounds superconductivity.

While thermogravimetric analysis have shown that the concentration of oxygen decreases after the reduction process,[9–13] there is no consensus about which oxygens are removed. Both Rietveld analysis of neutron powder diffraction[14–16] and EXAFS (Ref. 17) have concluded that CuO_2 in plane O(1) and out-of-plane O(2) oxygen vacancies are present in reduced Nd_2CuO_4. On the other hand, Pr_2CuO_4, Nd_2CuO_4, and $Nd_{2-x}Ce_xCuO_4$ neutron elastic scattering studies reported that only O(1) oxygen vacancies were created by the usual sample reduction.[18,19] In contrast to these results, no oxygen vacancies were detected by Mössbauer spectroscopy on samples with low $Cu \rightarrow {}^{57}Co$ substitution.[20] However, this technique suggested that a certain amount of apical oxygen O(3) is present in undoped samples, a suggestion that remains controversial. While some neutron measurements[16,18] concluded that Nd_2CuO_4 contains no apical oxygen, an apical oxygen site occupancy of 0.1 and 0.04 per formula unit has been reported by others[15] for oxygenated and reduced Nd_2CuO_4 samples, respectively. Further studies have proposed that the apical oxygen occupancy is reinforced with Ce-doping[9,17,19] and it has been claimed that the amount of O(3) removed by the reduction process decreases with Ce-doping.[11] Moreover, the Néel temperature of the as-grown samples decreases after reduction, as shown by neutron measurements,[21–23] particularly for $x \geqslant 0.1$.[22,23] Understanding how such small variations of the oxygen content induces dramatic changes in the transport and magnetic properties remains a crucial issue.

The rare earth (RE^{3+}) $4f$ electron crystal-field (CF) excitations, as established by Raman spectroscopy, infrared (IR) transmission, and inelastic neutron scattering, constitute a powerful local probe to investigate defects, as well as magnetic and electronic properties, particularly in the RE_2CuO_4 (Refs. 24–28) and $REBa_2Cu_3O_6$ (Refs. 29–32) systems (RE=Pr,Nd,Sm). This probe is also appropriate to the study of the oxygen nonstoichiometry in Ce-doped samples. A recent infrared transmission and Raman study of $Pr_{2-x}Ce_xCuO_4$ by Riou *et al.*[33] showed that the amount of apical oxygen increases with Ce-doping, and could not be removed by reduction of doped samples. Nevertheless, O(2) oxygen vacancies are created at low Ce-doping, while only O(1) oxygen vacancies appear for $x \geqslant 0.1$ following reduction. These surprising results are interpreted by the authors as the consequence of Ce-O(3) pair formation, which would favor the injection of holes in the CuO_2 planes. It is suggested that O(1) oxygen vacancies destroy the long-range antiferromagnetism and increase the carrier mobility.

Since $Nd_{2-x}Ce_xCuO_4$ compounds have been more extensively studied than $Pr_{2-x}Ce_xCuO_4$ samples, it is of great interest to confirm the mechanism of the reduction process, in order to interpret experimental results such as Hall coefficient measurements and ARPES data. In this paper, we present IR transmission and Raman studies of $Nd_{2-x}Ce_xCuO_4$ single crystals in order: (i) to characterize defects related to the oxygen nonstoichiometry and particularly to the presence of apical oxygen, (ii) to generalize the conclusions reported by Riou *et al.* in the $Pr_{2-x}Ce_xCuO_4$ compounds.[33]

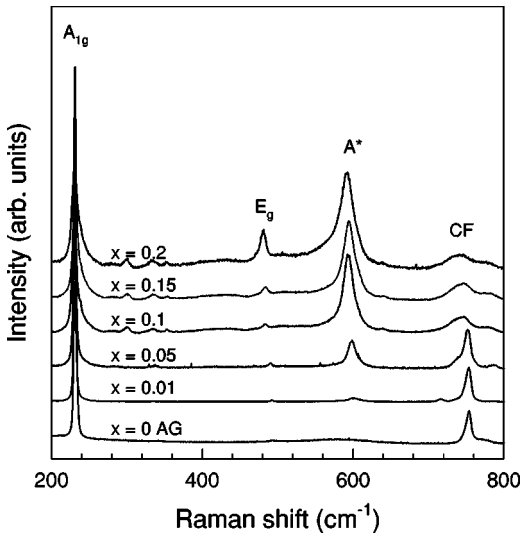

FIG. 1. Raman spectra at 7 K of oxygenated $Nd_{2-x}Ce_xCuO_4$ samples. AG corresponds to the as-grown sample while CF indicates a crystal-field excitation.

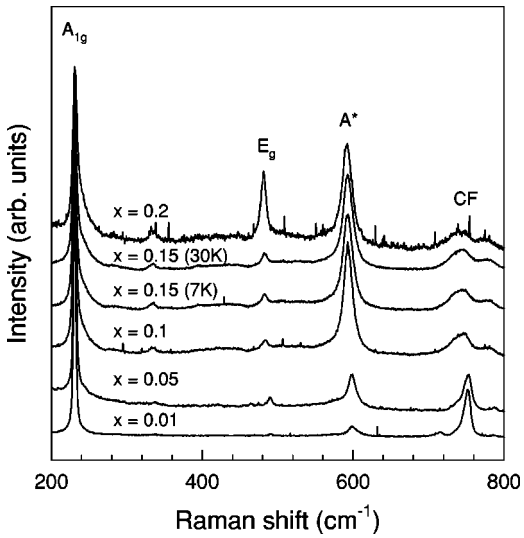

FIG. 2. Raman spectra at 7 K of reduced $Nd_{2-x}Ce_xCuO_4$ samples. CF indicates a crystal-field excitation.

II. EXPERIMENT

Single crystals of $Nd_{2-x}Ce_xCuO_4$ ($x=0, 0.005, 0.01, 0.05, 0.1, 0.15$, and 0.2) were grown by the flux technique.[34,35] In order to investigate oxygen nonstoichiometry, as-grown, reduced and oxygenated samples were studied. The as-grown samples were sandwiched between $Pr_{1.85}Ce_{0.15}CuO_4$ polycrystalline pellets[36] and reduced between 900 and 950 °C in Ar atmosphere. The same samples were subsequently oxygenated between 900 and 950 °C in O_2 atmosphere. The reduced $x=0.15$ has been found to be superconducting with a T_c of 22 K. Using a Fourier-transform interferometer (Bomem DA3.002) equipped with a CaF_2 beamsplitter, an InSb detector and both quartz and globar sources, 0.5 cm^{-1} resolution infrared transmission spectra were recorded at 9 K in the 1800–7000 cm^{-1} energy range. The samples were mounted with the c axis perpendicular to the unpolarized incident light beam. Raman spectra of the samples were also recorded between 150 and 800 cm^{-1} in the $x(zz)\bar{x}$ configuration using a Micro-Raman setup (Jobin-Yvon LabRam HR800) equipped with a He -Ne laser.

III. RESULTS

A. Raman spectroscopy

The Raman spectra of oxygenated and reduced $Nd_{2-x}Ce_xCuO_4$ samples are shown in Figs. 1 and 2, respectively. The Nd_2CuO_4 as-grown sample spectrum is presented together with the oxygenated sample spectra. Each spectrum has been normalized with respect to the Nd_2CuO_4 as-grown sample spectrum by calculating the surface ratio of the A_{1g} phonon peak at 231 cm^{-1}. This mode is not affected by the oxygen content since only rare earth ions are involved. This normalization procedure allows the determination of the A^* mode evolution as the Ce concentration is changed. This local mode, associated with apical oxygen in $Pr_{2-x}Ce_xCuO_4$,[33] is observed around 580 cm^{-1}, and its intensity increases with Ce-doping. The enhancement of the peak intensity mostly occurs at low doping, the integrated peak intensity remaining roughly constant for $x \geqslant 0.1$. Among the Ce-doped samples and the two undoped samples studies, only the Nd_2CuO_4 sample does not show the A^* mode, suggesting the absence of oxygen in apical position in this sample. It is worthwhile to note that the superconducting $x=0.15$ sample exhibits the same spectra at 30 K and 7 K. This suggests that no strong lattice deformation is observed as the sample enters the superconducting regime. In agreement with $Pr_{2-x}Ce_xCuO_4$ study,[33] the A^* local mode is not affected by the reduction in the Ce-doped samples. Hence, the presence of Ce adds tightly bound apical oxygens in $Nd_{2-x}Ce_xCuO_4$ as well as in $Pr_{2-x}Ce_xCuO_4$.

B. Infrared transmission

The CF interaction, that splits the Nd^{3+} free ion energy multiplets, is described by the Hamiltonian $H_{CF}=\Sigma B_{kq}C_q^{(k)}$.[37] The $(2k+1)$ operators $C_q^{(k)}$ $(q=k, k-1, \cdots, -k)$ are the components of a rank k irreducible tensor and the B_{kq} coefficients represent the CF parameters. To each Nd^{3+} environment corresponds a particular set of B_{kq} and its associated energy levels. The energies and symmetries of the CF multiplet levels, as well as the infrared selection rules resulting from the Nd^{3+} C_{4v} symmetry site in Nd_2CuO_4,[26] are used as templates to identify the corresponding absorption bands in the $Nd_{2-x}Ce_xCuO_{4\pm\delta}$ spectra. Additional absorption bands are associated with Nd^{3+} ions in nonregular sites.

The additional Nd^{3+} CF excitations related to the oxygen nonstoichiometry are reported in Table I. They are associated with Nd^{3+} ions located in the vicinity of either a defect produced by reduction or an apical oxygen. They correspond, respectively, to CF excitations whose relative intensities, with respect to the regular site, decrease or increase with the oxygen content. If the amount of a particular oxygen nonstoichiometry defect is neither modified by the reduction nor

TABLE I. Observed CF transitions (in cm^{-1}) corresponding to Nd^{3+} ions neighbored by an oxygen nonstoichiometry defect. The α, β, γ_1, and γ_2 defects, as well as the unassigned transitions, are related to the reduction process (see the text).

Multiplet	α	β	γ_1	γ_2	Unassigned	Apical oxygen
	1931	1893	1915	1902		1975
$^4I_{11/2}$	1966		1959	1906		2039
	2031		2210			2061
	2295		2265			2364
	3843		3879	3866		3897
	3890		4154	4168		3936
$^4I_{13/2}$	3982		4275	4194		3993
	4005					4302
	4025					4371
					5772	5848
					5788	5898
					5802	6380
					5821	6435
$^4I_{15/2}$					5835	6549
					6201	6603
					6229	
					6282	
					6332	

by the oxygenation of the samples, on needs to identify differently the corresponding transitions. This was done for the apical oxygen, as explained below. The intensities of the Nd^{3+} nonregular excitation associated with a particular defect are proportional to the defect density in a given sample. Hence, different defects may be distinguished if they do not appear in the same proportion in each sample. This allows us to group the absorption bands associated with removal of oxygen into four sets related to four distinct defects. Within a set, transitions have relative intensities that remain constant, and their absolute intensities vary proportionally to the corresponding defects, density. The groups of absorption bands, as well as the corresponding defects, are labeled α, β, γ_1, and γ_2. The nature of these defects is discussed in the next section. Each spectrum has been normalized with respect to the Nd_2CuO_4 as-grown spectrum using the intensity ratio of the spectra at appropriate free-absorption frequencies. Even though the undetermined dependence of the oscillator strength of the transitions associated with defects does not allow a quantitative analysis, important qualitative observations can be done. The low *c*-axis superconducting plasma frequency of cuprates[41] allows the infrared transmission through *ac*-planes in the superconducting state of the optimally doped sample.

As typical results, Figs. 3 and 4 display, respectively, for various Ce contents, the Nd^{3+} ion $^4I_{9/2} \rightarrow {}^4I_{11/2}$ transitions (8.5 K) of the oxygenated and reduced samples. The conclusion obtained by the analysis of these spectra remains for the $^4I_{9/2} \rightarrow {}^4I_{13/2}$ and $^4I_{9/2} \rightarrow {}^4I_{15/2}$ spectral ranges ($3500-7000\ cm^{-1}$). The transitions related to oxygen nonstoichiometry defects between 1800 and 7000 cm^{-1} are reported in Table I. Transitions occurring in spectral ranges where the signal to noise ratio is too weak, have not been assigned to a particular defect. The CF transitions related to Nd^{3+} ion in the proximity of an apical oxygen are indicated in Figs. 3 and 4 by solid lines, those referring to a Nd^{3+} ion

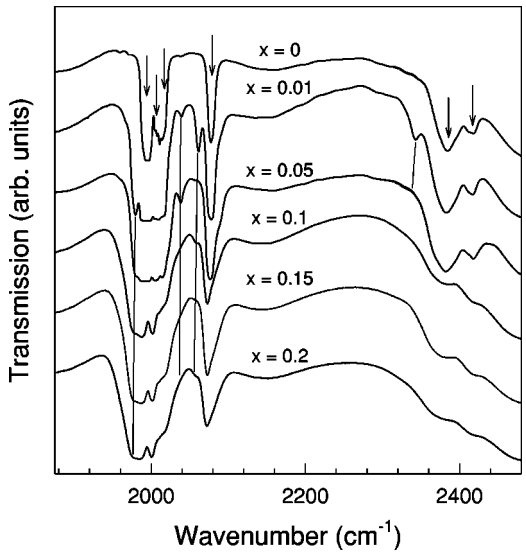

FIG. 3. Nd^{3+} $^4I_{9/2} \rightarrow {}^4I_{11/2}$ low temperature (8.5 K) infrared transmission CF excitations of the oxygenated $Nd_{2-x}Ce_xCuO_4$ samples. Downward arrows correspond to regular site Nd^{3+} CF excitations while solid line indicate CF excitations of Nd^{3+} in the vicinity of an apical oxygen.

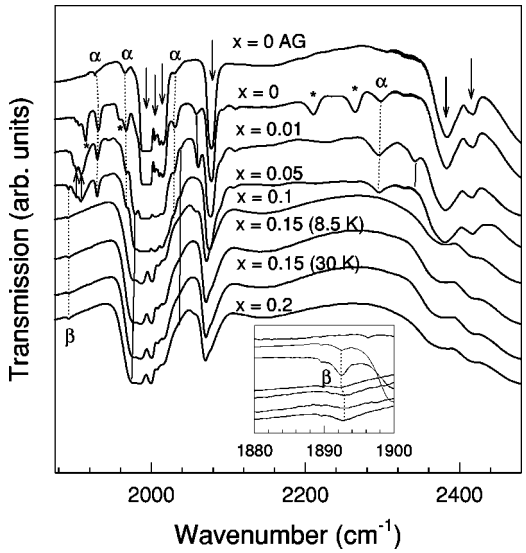

FIG. 4. Nd^{3+} $^4I_{9/2} \rightarrow {}^4I_{11/2}$ low temperature (8.5 K) infrared transmission CF excitations of the reduced $Nd_{2-x}Ce_xCuO_4$ samples. Downward arrows correspond to regular site Nd^{3+} CF excitations, while solid and dotted lines indicate CF excitations of Nd^{3+} in the vicinity of an apical oxygen and an oxygen vacancy, respectively (α and β refer to oxygen vacancies out and in the CuO_2 planes, respectively). Upward arrows and asterisks are, respectively, related to the γ_2 and γ_1 defects (see the text). The curves in the inset correspond, from top to bottom, to the samples: $x=0$ (as-grown), $x=0.01$, $x=0.05$, $x=0.1$, $x=0.15$ (8.5 K), $x=0.15$ (30 K), $x=0.2$.

in the vicinity of α and β defects are indicated by dotted lines, and the CF excitations associated with the γ_1 and γ_2 defects are identified by asterisks and upward arrows, respectively.

The C_{4v} regular site absorption bands, observed at 1995, 2006, 2013, 2077, 2383, and 2414 cm^{-1} in Nd_2CuO_4, as shown in Figs. 3 and 4, are not affected by the oxygen content, indicating that the main structure remains the same. Following Ce-doping, these CF excitations are broadened by the disorder introduced by the randomly distributed Ce^{4+} ions, and shift slightly, due to small variations of the lattice parameters. Additional absorption bands indicate the presence of local defects. Nonregular site CF transitions observed in the oxygenated samples are also observed in the reduced samples with the same relative intensities to the regular site transitions. These CF excitations, detected around 1975, 2039, 2061, and 2364 cm^{-1}, which do not vary with the oxygen content, are enhanced and broadened with Ce-doping. A direct correlation between these transitions, observed in all sample spectra except Nd_2CuO_4, and the A^* local mode observed by Raman scattering in the same samples, indicates that these CF absorption bands are associated with Nd^{3+} ions in the vicinity of an apical oxygen. Their intensities do not vary after either the reduction or the oxygenation processes, confirming that these processes do not change the amount of apical oxygen, as observed with Raman spectroscopy in $Nd_{2-x}Ce_xCuO_4$ (see Sec. III A) and $Pr_{2-x}Ce_xCuO_4$.[33]

The CF excitations observed in the reduced samples, which are absent following their oxygenation, are associated with the reduction process. Four sets of such transitions may be distinguished. The transitions at 1931, 1966, 2031, and 2295 cm^{-1}, which have the same relative intensities in each spectrum, are assigned to the α set. While they are detected in the as-grown Nd_2CuO_4 spectra as well as in all the $Nd_{2-x}Ce_xCuO_4$ reduced sample spectra for $x<0.1$, they are not observed in the reduced sample spectra for higher Ce content. The only transition observed after reduction in the $x\geqslant 0.1$ samples is detected at 1893 cm^{-1} and is ascribed to the β defect. This defect is present in the reduced samples for $x\geqslant 0.01$, as can be seen in the inset of Fig. 4. The weakness of this absorption band suggests that the corresponding defect density is small. Two additional sets of transitions related to the reduction process, which behave differently from the α and β type transitions, are found in some reduced samples. The transitions at 1915, 1959, 2210, and 2265 cm^{-1}, detected in reduced Nd_2CuO_4 and weakly in reduced $Nd_{1.99}Ce_{0.01}CuO_4$ only, are assigned as γ_1 defect transitions and those observed at 1902 and 1906 cm^{-1} as γ_2 defect transitions. While the latter defect is present in the reduced sample with $x\leqslant 0.05$, it is absent in the highly doped sample after reduction. It is worthwhile to note that the superconducting $x=0.15$ reduced sample spectra obtained below and above T_c are identical, suggesting that no strong local structural deformation occurs as the sample enters the superconducting state.

IV. DISCUSSION

Despite the influence of Ce-doping and thermal treatments on the sample infrared spectra, the main site CF excitation energies of all samples do not vary significantly with the oxygen and the Ce contents. The small energy variations are due to slight modifications of the lattice parameters. This indicates that there are no long range distortions following Ce-doping and thermal treatments of as-grown samples. Defects affect the structure only locally and manifest themselves by the presence, in the various spectra, of additional sharp Nd^{3+} CF absorption bands. We can also conclude, from this observation, that the reduction and the oxygenation processes lead to very small changes in the oxygen content of the samples. Unfortunately, it is not possible to determine the precise value of the oxygen content since the transition oscillator strengths depend on the defect environment. Nevertheless, our qualitative analysis leads to some fundamental conclusions concerning the impact of the reduction process.

In contrast to the observation in Pr_2CuO_4,[33] no excitation in the Nd_2CuO_4 Raman or the infrared transmission spectra has been removed after the reduction of the samples or enhanced by the oxygenation process. However $Nd_{2-x}Ce_xCuO_4$ Raman spectra exhibit the same A* Raman mode that has been clearly related to the presence of apical oxygens in $Pr_{2-x}Ce_xCuO_4$. Hence, the presence of apical oxygens in these samples is confirmed. The Nd_2CuO_4 sample is apical oxygen free since its Raman spectra do not show the A* mode. In agreement with the $Pr_{2-x}Ce_xCuO_4$ results, the $Nd_{2-x}Ce_xCuO_4$ A^* Raman mode intensity, and the corresponding amount of O(3), increases with Ce-doping. As shown for the $Pr_{2-x}Ce_xCuO_4$ compounds, these particular oxygens could not be removed by reduction in the doped $Nd_{2-x}Ce_xCuO_4$ samples. This also suggests that the Pr_2CuO_4 compound, at the frontier of the $T'\rightarrow T$ structural transition, allows more easily distortions, which favor the introduction of extraneous oxygens in the apical position, than does Nd_2CuO_4.

In agreement with the $Pr_{2-x}Ce_xCuO_4$ data,[33] a direct correlation between the A* Raman mode and a particular Nd^{3+} nonregular site may be established. Similarly to the $Nd_{2-x}Ce_xCuO_4$ A* Raman mode, the CF excitations related to this site are not affected by both oxygenation and reduction process. Moreover, the corresponding absorption bands, absent Nd_2CuO_4, increase with Ce-doping. This Nd^{3+} nonregular site, previously observed in the Ce-doped Nd_2CuO_4 (Ref. 38) and $Nd_{2-x}Ce_xCuO_4$ (Ref. 40) samples, has been attributed to charge inhomogeneities being reinforced by the Ce-doping. The recent results obtained on $Pr_{2-x}Ce_xCuO_4$, as well as the assumption that the physical properties of $Pr_{2-x}Ce_xCuO_4$ and $Nd_{2-x}Ce_xCuO_4$ are closely related, attribute the origin of these inhomogeneities to apical oxygens. Actually, recent *ab initio* calculations have shown that in the cuprates, the oxygen configuration surrounding the RE^{3+} are mostly responsible for the local CF at the RE^{3+} regular site.[39] The presence of apical oxygens strongly disturbs this oxygen configuration. Hence, if O(3) oxygen are present, they should be detected with Nd^{3+} CF excitations. This is the case because the ratio of the A^* to A_{1g} Raman peak integrated intensity is of the same order of magnitude in $Nd_{1.85}Ce_{0.15}CuO_4$ and $Pr_{1.85}Ce_{0.15}CuO_4$, indicating that the amount of apical oxygen is roughly the same in both compounds. Moreover, a defect easily detected with Pr^{3+} CF excitations in $Pr_{2-x}Ce_xCuO_4$, should also be detected in

$Nd_{2-x}Ce_xCuO_4$ using the CF excitations of the Nd^{3+} ions located in the same low symmetry nonregular sites.

While O(3) apical oxygens are neither introduced nor removed by thermal treatments, these processes are able to create and remove O(1) and O(2) oxygen vacancies. Two inequivalent oxygen sites are involved in the so-called T′ crystal structure of Nd_2CuO_4. Contrary to the $Pr_{2-x}Ce_xCuO_4$ samples where only two defects related to the reduction process are observed,[33] the four observed CF excitation sets related to the reduction process confirm the presence of four different defects. According to EXAFS (Ref. 17) and to neutron diffraction structural refinement results,[14–16] both defects corresponding to O(1) and O(2) oxygen vacancies are present in the reduced samples. Detected only in two samples, the γ_1 defect should not *a priori* be related to one of these oxygen vacancies. As observed in the $Pr_{2-x}Ce_xCuO_4$ compounds, the oxygen removed by the reduction process is not the same at low and high dopings. Only the β-defect is observed at high doping, and thus it must be related to an oxygen vacancy in one of the two regular sites. Consequently, the order oxygen vacancy type corresponds to either the α or the γ_2 defects. The sharpness of the α-type transitions as compared to the γ_2-type suggests that the α defect corresponds to an oxygen vacancy in a regular site. Also, since only a small amount of oxygen is removed by the reduction process,[9,11,15] the probability to detect CF transitions of a RE^{3+} in the neighborhood of two oxygen vacancies or more, is small. However, this possibility is not excluded in the case of γ_1 defects, present only in the reduced samples where the oxygen contents are the lowest (reduced Nd_2CuO_4 and $Nd_{1.99}Ce_{0.01}CuO_4$), i.e., the sample having the strongest transitions related to the reduction process.

The striking fact emerging from the $Pr_{2-x}Ce_xCuO_4$ and the $Nd_{2-x}Ce_xCuO_4$ studies is that the mechanism of reduction is not the same at low and high doping, and in contrast to the common belief, apical oxygen, although present, is not involved in this mechanism, except for the Pr_2CuO_4 compound. *The key role of* the *reduction proess, which triggers superconductivity in the so-called electron-doped superconductors, is to create oxygen vacancies rather than to remove apical oxygen*. The Madelung potentials calculated for sites O(1) and O(2) in the undoped compound indicate that oxygen ions are less strongly bound in the O(2) site than in the O(1) site.[3] Hence, the oxygen removed at low doping, associated with the α defect, corresponds to the O(2) position, while the oxygen removed at high doping, labeled as β defects, is located in the CuO_2 planes O(1) position. It is important to mention that all these defects related to the reduction process (α, β, γ_1, and γ_2) have disappeared after oxygenation of the samples, as confirmed by infrared transmission. This is an indication that they do not correspond to decomposition phases, such as the $(Nd,Ce)_2O_3$ epitaxial phase reported elsewhere.[42]

The reason why such a tiny amount of oxygen in the CuO_2 planes has to be removed in order to render the samples superconducting is not obvious. However, the appearance of superconductivity must be somehow related to the oxygen nonstoichiometry, since the reduction process is needed. A parallel between the structural defects, Hall coefficient measurements, and ARPES gives some hints. As suggested by the oxygen nonstoichiometry defects, $Nd_{2-x}Ce_xCuO_4$ compounds show two regimes, one at low doping dominated by the O(2) vacancies, and another one at high doping, for which apical oxygens and O(1) vacancies prevail. Similarly, the temperature dependence of the Hall coefficient is significantly different at low and high doping. While the Hall coefficient of lightly doped $Nd_{2-x}Ce_xCuO_4$ is negative and roughly temperature independent,[43] it gets a holelike component character for the reduced $Nd_{2-x}Ce_xCuO_4$ samples when Ce-doping becomes important. Hence, the Hall coefficient of $Nd_{1.85}Ce_{0.15}CuO_4$, although remaining negative, has a pronounced upturn once reduced.[7] Moreover, overdoped samples exhibit positive Hall coefficient.[8] Presence of holes at high Ce-doping, in the reduced samples, is confirmed by APRES.[44] Hence, a holelike Fermi surface centered at $(\pi/2, \pi/2)$, that could be reinforced by the reduction process, appears at high doping.

The oxygen nonstoichiometry defects observed in this study lead to two possible scenarios for the injection of holelike carriers in the CuO_2 planes. The first one concerns the formation of Ce-O (3) pairs.[33] O(1) vacancies would then affect the long range antiferromagnetism. Although the amount of apical oxygen is enhanced with Ce-doping, it is not obvious to determine what proportion of Ce produces Ce–O(3) pairs. The second scenario can be understood using the Hubbard model and the modification of the Fermi surface. As doping increases, the Hubbard gap is reduced until the Fermi level crosses both the upper Hubbard band around $(\pi, 0)$ and the top of the lower Hubbard band at $(\pi/2, \pi/2)$.[45] The presence of Ce^{4+} ions in substitution to Nd^{3+} ions increases the stability of the O(2) oxygen with respect to O(1), allowing preferentially the creation of O(1) vacancies. Such vacancies, even though in small proportion, are the likely candidates to affect sufficiently the long range antiferromagnetism and the shape of the Hubbard bands. They prevail for $x \geqslant 0.1$, the doping range for which a large decrease of Néel temperature after reduction is observed.[22,23] Furthermore, as long as antiferromagnetic fluctuations persist, these holelike carriers, located on the first magnetic Brillouin zone, could be coupled with antiferromagnetic wave vector $\mathbf{Q}=(\pi, \pi)$. The antiferromagnetic fluctuations would then be responsible for the formation of Cooper pairs, as suggested by STS results on $Bi_2Sr_2CaCu_2O_{8+\delta}$, which show that superconductivity is locally destroyed by the substitution of Cu^{2+} with nonmagnetic Zn^{2+},[46] while unaffected by substitution of Cu^{2+} with magnetic Ni^{2+}.[47] This is consistent with theoretical calculations which indicate that antiferromagnetic fluctuations enhance *d*-wave pairing correlations.[48] In summary, these scenarios question the nature of the superconducting carriers in the electron-doped cuprates, as well as the eventual asymmetry between electrons and holes in the pairing mechanism in these materials.

V. CONCLUSION

In this study, we have shown that Raman scattering and CF infrared transmission spectroscopy are powerful tools for characterizing defects related to oxygen nonstoichiometry in

$Nd_{2-x}Ce_xCuO_4$ samples. The results obtained in these compounds are in good agreement with a recent study of $Pr_{2-x}Ce_xCuO_4$ by Riou *et al.*[33] The Nd^{3+} regular sites are neither affected significantly by the oxygen content, nor by the Ce content. Also, the reduction process of the samples, which triggers superconductivity in these materials, is not the same at high and low doping. Oxygen vacancies in the O(2) sites are created following reduction of low Ce-doping samples while O(1) vacancies are created at high Ce-doping samples. Contrary to the widespread belief, the amount of apical oxygen, that increases with Ce-doping, is not affected by the reduction process. We have also proposed scenarios by which holelike carriers are injected in the CuO_2 planes, in agreement with Hall coefficient measurements and ARPES.

ACKNOWLEDGMENTS

We thank J. Rousseau and M. Castonguay for technical assistance. We also acknowledge support from the National Sciences and Engineering Research Council of Canada (NSERC), le Fonds Québécois de la Recherche sur la Nature et les Technologies du Gouvernement du Québec and the Canadian Institue for Advanced Research.

*Electronic address: prichard@physique.usherb.ca

[1] Y. Tokura, H. Takagi, and S. Uchida, Nature (London) **337**, 345 (1989).
[2] M. Brinkmann, T. Rex, M. Steif, H. Bach, and K. Wasterholt, Physica C **269**, 76 (1996).
[3] J. E. Hirsch, Physica C **243**, 319 (1995).
[4] Z. Z. Wang, T. R. Chien, N. P. Ong, J. M. Tarascon, and E. Wang, Phys. Rev. B **43**, 3020 (1991).
[5] W. Jiang, S. N. Mao, X. X. Xi, X. Jiang, J. L. Peng, T. Venkatesan, C. J. Lobb, and R. L. Greene, Phys. Rev. Lett. **73**, 1291 (1994).
[6] P. Fournier, P. Mohanty, E. Maiser, S. Darzens, T. Venkatesan, C. J. Lobb,G. Czjzek,R. A. Webb, and R. L. Greene, Phys. Rev. Lett. **81**, 4720 (1998).
[7] P. Fournier, X. Jiang, W. Jiang, S. N. Mao, T. Venkatesan, C. J. Lobb, and R. L. Greene, Phys. Rev. B **56**, 14149 (1997).
[8] P. Fournier, E. Maiser, and R. L. Greene, *The Gap Symmetry and Fluctuations in High-T_c Superconductors*, edited by Bok *et al.* (Plenum, New York, 1998).
[9] E. Moran, A. I. Nazzal, T. C. Huang, and J. B. Torrance, Physica C **160**, 30 (1989).
[10] J. S. Kim and D. R. Gaskell, Physica C **209**, 381 (1993).
[11] E. Wang, J.-M. Tarascon, L. H. Greene, G. W. Hull, and W. R. McKinnon, Phys. Rev. B **41**, 6582 (1990).
[12] W. Takayama-Muromachi, F. Izumi, Y. Uchida, K. Kato, and H. Asano, Physica C **159**, 634 (1989).
[13] K. Susuki, K. Kishio, T. Hasegawa, and K. Kitazawa, Physica C **166**, 357 (1990).
[14] F. Izumi, Y. Matsui, H. Takagi, S. Uchida, Y. Tokura, and H. Asano, Physica C **158**, 433 (1989).
[15] P. G. Radaelli, J. D. Jorgensen, A. J. Schultz, J. L. Peng, and R. L. Greene, Phys. Rev. B **49**, 15322 (1994).
[16] C. Marin, J. Y. Henry, and J. X. Boucherie, Solid State Commun. **86**, 425 (1993).
[17] B. D. Padalia, G. S. Okram, O. Prakash, S. J. Gurman, and J. C. Amiss, J. Phys.: Condens. Matter **9**, 9695 (1997).
[18] P. Vigoureux, W. Paulus, M. Barden, A. Cousson, G. Hegger, J. Y. Henry, V. Kvardakov, A. Ivonov, and P. Galez, Physica C **235–240**, 1263 (1994).
[19] P. Vigoureux, W. Paulus, J. Y. Henry, S. Piñol, and G. Heger, Physica B **234–236**, 719 (1997).
[20] V. Chechersky, N. S. Kopolev, O. Beom-hoan, M. I. Larkin, J.-L. Peng, J. T. Market, R. L. Greene, and A. Nath, Hyperfine Interact. **93**, 1721 (1994).
[21] M. Matsuda, Y. Endoh, K. Yamada, H. Kojima, I. Tanaka, R. J. Birgeneau, M. A. Kastner, and G. Shirane, Phys. Rev. B **45**, 12548 (1992).
[22] T. Uefuji, K. Kurahashi, M. Fujita, M. Matsuda, and K. Yamada, Physica C **378–381**, 273 (2002).
[23] P. K. Mang. O. P. Vajk, A. Arvanitaki, J. W. Lynn, and M. Greven, cond-mat/0307093 (2003).
[24] S. Jandl, T. Strach, T. Ruf, M. Cardona, V. Nekvasil, M. Iliev, D. I. Zhigunov, S. N. Barilo, and S. V. Shiryaev, Phys. Rev. B **56**, 5049 (1997).
[25] G. Riou, S. Jandl, M. Poirier, V. Nekvasil, M. Diviš, P. Fournier, R. L. Greene, D. I. Zhigunov, and S. N. Barilo, Eur. Phys. J. B **23**, 179 (2001).
[26] S. Jandl, P. Dufour, P. Richard, V. Nekvasil, D. I. Zhigunov, S. N. Barilo, and S. V. Shiryaev, J. Lumin. **78**, 197 (1998).
[27] S. Jandl, P. Richard, V. Nekvasil, D. I. Zhigunov, S. N. Barilo, and S. V. Shiryaev, Physica C **314**, 189 (1999).
[28] A. T. Boothroyd, S. M. Doyle, D. M. Paul, and R. Osborn, Phys. Rev. B **45**, 10075 (1992).
[29] A. A. Martin, T. Ruf, T. Strach, M. Cardona, and T. Wolf, Phys. Rev. B **58**, 14349 (1998).
[30] A. A. Martin, T. Ruf, M. Cardona, S. Jandl, D. Barba, V. Nekvasil, M. Deviš, and T. Wolf, Phys. Rev. B **59**, 6528 (1999).
[31] D. Barba, S. Jandl, V. Nekvasil, M. Maryško, M. Diviš, A. A. Martin, C. T. Lin, M. Cardona, and T. Wolf, Phys. Rev. B **63**, 054528 (2001).
[32] M. Guillaume, W. Henggeler, A. Furrer, R. S. Eccleston, and V. Trounov, Phys. Rev. Lett. **74**, 3423 (1995).
[33] G. Riou, P. Richard, S. Jandl, M. Poirier, P. Fournier, V. Nekvasil, S. N. Barilo, and L. A. Kurnevich, Phys. Rev. B **69**, 024511 (2004).
[34] S. N. Barilo and D. N. Zhigunov, Supercond., Phys. Chem. Technol. **2**, 138 (1989).
[35] S. J. Hagen, J. L. Peng, Z. Y. Li, and R. L. Greene, Phys. Rev. B **43**, 13606 (1991).
[36] M. Brinkmann, T. Rex, H. Bach, and K. Westerholt, J. Cryst. Growth **163**, 369 (1996).
[37] B. R. Judd, *Operator Techniques in Atomic Spectroscopy* (McGraw–Hill, New York, 1963).
[38] S. Jandl, P. Richard, M. Poirier, V. Nekvasil, A. A. Nugroho, A. A. Menovsky, D. I. Zhigunov, S. N. Barilo, and S. V. Shiryaev, Phys. Rev. B **61**, 12882 (2000).

[39] M. Diviš and V. Nekvasil, J. Alloys Compd. **323–324**, 567 (2001).
[40] P. Richard, S. Jandl, Z. Ichalalene, M. Poirier, V. Nekvasil, C. T. Lin, and M. Cardona, Physica C **341**, 2145 (2000).
[41] K. Tamasaku, Y. Nakamura, and S. Uchida, Phys. Rev. Lett. **69**, 1455 (1992).
[42] M. Matsuura, P. Dai, H. J. Kang, J. W. Lynn, D. N. Argyriou, K. Prokes, Y. Onose, and Y. Tokura, Phys. Rev. B **68**, 144503 (2003).
[43] P. Fournier (private communication).
[44] N. P. Armitage, F. Ronning, D. H. Lu, C. Kim, A. Damascelli, K. M. Shen, D. L. Feng, H. Eisaki, Z.-H. Shen, P. K. Mang, N. Kaneko, M. Greven, Y. Onose, Y. Taguchi, and Y. Tokura, Phys. Rev. Lett. **88**, 257001 (2002).
[45] C. Kusko, R. S. Markiewicz, M. Lindroos, and A. Bansil, Phys. Rev. B **66**, 140513 (2002).
[46] S. H. Pan, E. W. Hudson, K. M. Lang, H. Eisaki, S. Uchida, and J. C. Davis, Nature (London) **403**, 746 (2000).
[47] E. W. Hudson, K. M. Lang, V. Madhavan, S. H. Pan, H. Eisaki, S. Uchida, and J. C. Davis, Nature (London) **411**, 920 (2001).
[48] B. Kyung, J.-S. Landry, and A.-M. S. Tremblay, Phys. Rev. B **68**, 174502 (2003).